Available online at www.sciencedirect.com
ScienceDirect
Journal of Solid State Chemistry 181 (2008) 20–29
JOURNAL OF SOLID STATE CHEMISTRY
www.elsevier.com/locate/jssc

Energetics of formation of alkali and ammonium cobalt and zinc phosphate frameworks

So-Nhu Le, Alexandra Navrotsky*

Peter A. Rock Thermochemistry Laboratory, Chemistry Department, NEAT ORU, University of California at Davis, Davis, CA 95616, USA

Received 18 July 2007; received in revised form 10 October 2007; accepted 16 October 2007
Available online 22 October 2007

Abstract

Alkali and ammonium cobalt and zinc phosphates show extensive polymorphism. Thermal behavior, relative stabilities, and enthalpies of formation of $KCoPO_4$, $RbCoPO_4$, NH_4CoPO_4, and NH_4ZnPO_4 polymorphs are studied by differential scanning calorimetry, high-temperature oxide melt solution calorimetry, and acid solution calorimetry.

α-$KCoPO_4$ and γ-$KCoPO_4$ are very similar in enthalpy. γ-$KCoPO_4$ slowly transforms to α-$KCoPO_4$ near 673 K. The high-temperature phase, β-$KCoPO_4$, is 5–7 kJ mol^{-1} higher in enthalpy than α-$KCoPO_4$ and γ-$KCoPO_4$. HEX phases of NH_4CoPO_4 and NH_4ZnPO_4 are about 3 kJ mol^{-1} lower in enthalpy than the corresponding ABW phases. There is a strong relationship between enthalpy of formation from oxides and acid–base interaction for cobalt and zinc phosphates and also for aluminosilicates with related frameworks. Cobalt and zinc phosphates exhibit similar trends in enthalpies of formation from oxides as aluminosilicates, but their enthalpies of formation from oxides are more exothermic because of their stronger acid–base interactions. Enthalpies of formation from ammonia and oxides of NH_4CoPO_4 and NH_4ZnPO_4 are similar, reflecting the similar basicity of CoO and ZnO.
© 2007 Elsevier Inc. All rights reserved.

Keywords: Enthalpy of formation; Phase transformation; Cobalt phosphate framework; Zinc phosphate framework; $KCoPO_4$; $RbCoPO_4$; NH_4CoPO_4; NH_4ZnPO_4

1. Introduction

Transition metal phosphates, such as $ACoPO_4$ (A = Na, K, Rb, NH_4^+) [1], $NaZnPO_4$ [2], NH_4ZnPO_4 [3,4], $(H_3NCH_2CH_2NH_3)_{0.5}CoPO_4$ [5,6], $(H_3N(CH_2)_3NH_3)_{0.5}ZnPO_4$ [7], $[C_5N_2H_{14}][Zn_2(PO_3(OH))_3]$ [8], $[C_8N_5H_{28}][Zn_5(PO_4)_5]H_2O$ [9], $[C_2N_2H_{10}]_2[Co_4(PO_4)_4]H_2O$ [10], have attracted great interest in the last decade because of their potential to form framework structures similar to aluminosilicate zeolites. Several studies have been devoted to thermodynamics of the formation of pure silica, aluminosilicate, and aluminophosphate zeolites to gain insight into their fundamental structures, bonding, stability and synthesis conditions [11–15]. An initial study of the thermodynamics of transition metal phosphates, aimed at different polymorphs of $NaCoPO_4$ [16], found results analogous to those for zeolitic materials, namely that the enthalpy differences among several $NaCoPO_4$ polymorphs are small. However, cobalt is stable in an octahedral environment and acid–base interactions in $NaCoPO_4$ are much stronger than those in aluminosilicates. In order to obtain a more comprehensive picture of the energetics of transition metal phosphates, this study investigates thermodynamics of formation of $KCoPO_4$, $RbCoPO_4$, NH_4CoPO_4, and NH_4ZnPO_4.

All compounds in this study have frameworks constructed from alternation of CoO_4 and PO_4 or ZnO_4 and PO_4 tetrahedra. $RbCoPO_4$ crystallizes in the $P2_1$ space group and has the ABW zeolite framework with channels of eight-member rings and six-member rings in two directions [1] (the three-letter code designates the specific framework topology of zeolite structure [17]). Neither phase transitions nor other polymorphs of this compound have been reported. Three polymorphs of $KCoPO_4$ are known. α-$KCoPO_4$ crystallizes in the $P6_3$ space group, and is isostructural with β-$NaCoPO_4$ [1,18]. This structure is denoted as HEX and has six-member ring channels in one

*Corresponding author. Fax: +1 530 752 9307.
E-mail address: anavrotsky@ucdavis.edu (A. Navrotsky).

0022-4596/$ - see front matter © 2007 Elsevier Inc. All rights reserved.
doi:10.1016/j.jssc.2007.10.017

direction. It undergoes a phase transition to β-$KCoPO_4$ (the high-temperature phase) at 849 K [19–21]. That phase is orthorhombic with cobalt in a tetrahedral environment [20,21]; however, its detailed structure has not been determined. Upon cooling, β-$KCoPO_4$ undergoes a ferroelastic phase transition with the formation of γ-$KCoPO_4$, an incommensurate ferroelastic phase [20]. α-$KCoPO_4$ has been proposed to be a metastable phase and γ-$KCoPO_4$ the stable phase at ambient conditions. Ignoring the modulation of the incommensuration, the structure of γ-$KCoPO_4$ was solved within the space group $P2_1/c$ and is related to the tridymite structure [20].

Both NH_4CoPO_4 and NH_4ZnPO_4 are known in the HEX and the ABW frameworks mentioned above. NH_4^+ ions reside in six ring channels of the HEX or eight ring channels of the ABW phase. Ammonium cobalt and zinc phosphates crystallize in the $P2_1$ space group for the ABW structure, and in the $P6_3$ space group for the HEX structure [1,3,4].

Differential scanning calorimetry and high-temperature oxide melt solution calorimetry are used to study transformation behavior, relative stability of various $KCoPO_4$ polymorphs and enthalpy of formation of $KCoPO_4$ and $RbCoPO_4$. Since ammonium compounds decompose and release ammonia and/or nitrogen around 673 K, acid solution calorimetry at room temperature is used to determine relative stabilities of the HEX and ABW phases and enthalpy of formation of NH_4CoPO_4 and NH_4ZnPO_4. Acid–base interactions in cobalt and zinc phosphate compounds as well as their energetic trends compared to aluminosilicates are discussed based on these new thermodynamic data and our previous works [15,16,18].

2. Experiments

2.1. Sample preparation

Various methods were applied to make samples. Sources of chemicals used for syntheses are given in Table 1. α-$KCoPO_4$ was prepared by a modification of the hydrothermal method of Feng et al. [1]. Eight milliliters of deionized water and 1.35 mL of H_3PO_4 were mixed with 1.18 g of $CoCO_3 \cdot xH_2O$ (99.998% metals basis, Sigma–Aldrich). Carbon dioxide evolved during stirring. Then 8 mL of KOH solution was added; the pH of the mixture was 8.0. One milliliter of ethylenediamine was added and brought the pH to 10.5. Crystals of α-$KCoPO_4$ were obtained after heating the violet reaction mixture in a 23 mL Teflon-coated container in an autoclave at 443 K for 10 days.

Table 1
Sources of the chemicals used in syntheses

Chemical	Purity	Supplier
$CoCO_3 \cdot xH_2O$	>99.998% metals basis	Sigma–Aldrich
$Co(NO_3)_2 \cdot 6H_2O$	99% (assay)	Fluka
$Zn(CH_3COO)_2 \cdot 2H_2O$	98.0–101.0% (assay)	Alfa Aesar
H_3PO_4	⩾85% (assay)	Fisher Scientific
KOH	20% (CAS 1310-58-3)	LabChem Inc.
50% RbOH	99.6% metals basis	Alfa Aesar
Ammonium hydroxide	28–30% NH_3	Alfa Aesar
$(NH_4)_2CO_3$	30+% NH_3	Alfa Aesar
Ethylene glycol	99%	Alfa Aesar
1,4-Diaminobutane	98+%	Alfa Aesar
Ethylenediamine	50% solution	Alfa Aesar
Dimethyamine	99%	Alfa Aesar

γ-$KCoPO_4$ was prepared followed the method of Lujan and Schmid [20] by mixing α-$KCoPO_4$ and KCl in a 1:1 weight ratio and heating in a platinum crucible at 1173 K for four hours, then cooling at 0.15 K min^{-1} to room temperature. KCl was rinsed out of the crystallized product by washing the mixture with deionized water in an ultrasonic cleaner several times.

$RbCoPO_4$ was made by dissolving 2.9 g of $Co(NO_3)_2 \cdot 6H_2O$ into 9.0 mL of deionized water and 1.4 mL of H_3PO_4. An RbOH solution was added dropwise until pH reached 7.5. Then 0.5 mL of dimethylamine solution was added to bring the pH to 9.5. A blue violet powder of $RbCoPO_4$ was formed after heating the reactant mixture in an autoclave at 453 K for 8 days. All $KCoPO_4$ and $RbCoPO_4$ products were recovered by vacuum filtration, washed with deionized water, dried at 383 K in air, and kept in sealed vials placed in a desiccator containing $CaCl_2$.

HEX–NH_4CoPO_4 and ABW–NH_4CoPO_4 were prepared following the hydrothermal methods of Feng et al. [1]. To prepare HEX–NH_4ZnPO_4, 2.5 g of $(NH_4)_2CO_3$ was dissolved in 2 mL of water and 1.4 mL of H_3PO_4 to form solution A, and 1.1 g $Zn(CH_3COO)_2 \cdot 2H_2O$ was dissolved into 2.5 mL of deionized water to form solution B. Solutions A and B were mixed together in a Teflon bottle and kept at 343 K for 10 days, then hexagonal rod crystals of HEX–NH_4ZnPO_4 were recovered by vacuum filtration. ABW–NH_4ZnPO_4 was prepared by a method similar to that described by Bu et al. [3]. About 16 mL of ammonia solution was added to a solution of 0.8 g of $Zn(CH_3COO)_2 \cdot 2H_2O$ and 0.65 mL of H_3PO_4 in 22 mL of deionized water. The clear solution in a Teflon bottle was heated at 393 K for 2 days, then the irregular-shaped crystals of ABW–NH_4ZnPO_4 were recovered by vacuum filtration. These samples were dried at 383 K in air and kept in sealed vials placed in a desiccator containing $CaCl_2$.

In addition to the above samples, $NH_4H_2PO_4$, CoO, and ZnO were used as supplementary chemicals for thermodynamic cycle to determine enthalpies of formation (see below). Puratronic $NH_4H_2PO_4$ (99.999% metals basis) was purchased from Sigma–Aldrich. ZnO crystals were prepared by mixing 3 mL of ammonium hydroxide with the solution of 2.2 g $Zn(CH_3COOH)_2 \cdot 2H_2O$ in 5 mL of deionized water and heating in an autoclave with a Teflon liner at 443 K for 3 days. The preparation of CoO has been described elsewhere [22]. CoO, ZnO, and $NH_4H_2PO_4$ were ground and dried under vacuum at 393 K for calorimetric measurements.

2.2. Sample characterization

Powder X-ray diffraction (XRD) patterns were obtained on a Scintag PAD-V diffractometer operated at 45 kV and 40 mA with Cu$K\alpha$ radiation. Data were collected from 10° to 60° (2θ) with a step size of 0.02° (2θ) and a dwell time of 1 s for samples without cobalt and 2.5 s for samples with cobalt. The XRD pattern of CoO was collected from 30° to 90° (2θ)· Quartz was used as an external standard for diffractometer calibration. Simulated powder patterns from the ICSD database [23], or crystallographic data from single crystal and powder patterns [1,20] were used as references for phase identification. Lattice parameters were refined from XRD patterns using JADE software [24].

Chemical compositions of cobalt and zinc phosphate samples were determined by combination of thermogravimetric analysis (TGA, see below) and electron microprobe analysis. While TGA was used to check moisture in $KCoPO_4$ and $RbCoPO_4$, the weight losses from the TGA traces of ammonium cobalt and zinc phosphate correspond to their content of NH_3 and H_2O as represented by the following reaction:

$$NH_4MPO_4(cr) \rightarrow NH_3(g) + \tfrac{1}{2}H_2O(g) + \tfrac{1}{2}M_2P_2O_7(cr), \quad (1)$$

where M = Co or Zn.

$KCoPO_4$, $RbCoPO_4$, and the residues of ammonium cobalt and zinc phosphates after TGA experiments were palletized, annealed at 1273 K (for cobalt phosphates) or 1223 K (for zinc phosphates), and polished for microprobe analysis to determine contents of K, Rb, Co, Zn, and P. Analyses were performed on a Cameca SX-100 instrument. Orthoclase ($KAlSi_3O_8$), rubidium titanyl phosphate ($RbTiOPO_4$), cobalt metal, zinc metal, and apatite were used as standards for quantitative determination of K, Rb, Co, Zn, and P, respectively.

2.3. Thermogravimetric analysis (TGA) and differential scanning calorimetry (DSC)

Weight loss and thermal behavior of samples were investigated by TGA and DSC performed on a Netzsch STA 449 instrument. Pellets of approximately 50 mg in mass were heated in a platinum crucible from 303 to 1273 K in argon atmosphere with a heating rate of 10 K min^{-1}, and an argon flow rate of 40 cm^3 min^{-1}. Enthalpies of phase transitions of $KCoPO_4$ were studied by heating and cooling $KCoPO_4$ samples around the temperature of phase transitions on a Netzsch DSC 404 unit under the same conditions. Heat flow calibration was based on heat capacity of a corundum disk run in the same platinum crucible.

2.4. High-temperature oxide melt solution calorimetry

Enthalpies of formation of $KCoPO_4$ and $RbCoPO_4$ were derived by applying Hess's law (the first law of thermodynamics) to enthalpies of drop solution of samples and their component oxides in sodium molybdate melt solvent ($3Na_2O \cdot 4MoO_3$) at 973 K. A custom built Tian–Calvet twin calorimeter described elsewhere [25,26] was used to measure enthalpies of drop solution of $KCoPO_4$ and $RbCoPO_4$. Experiments were conducted under the same conditions as in our previous study of $NaCoPO_4$ [16].

2.5. Acid solution calorimetry

Relative stabilities of HEX and ABW structures and enthalpies of formation of ammonium cobalt and zinc phosphates were determined by applying Hess' law to the enthalpies of solution of samples and supplementary chemicals ($NH_4H_2PO_4$, CoO, and ZnO) in a 5 M HCl solution. Enthalpies of solution were measured on a commercial CSC 4400 isothermal microcalorimeter operated at 298 K. Samples were made into pellets of about 5–40 mg each (depending on heat of solution of compounds) and dropped into 25 g of 5 M HCl (standardized solution, VWR) in the calorimeter. At least six measurements were performed for each sample. Mechanical stirring was used to facilitate the solution. Calibration was performed by dissolving 15 mg pellets of KCl (NIST Standard Reference Material 1655 [27]) in 25 g of deionized water in the calorimeter at the same conditions; enthalpy of solution of KCl in water at 298 K was calculated and corrected to the reference state of $m = 0.008$ mol kg^{-1} following the Standard Reference Material 1655 [27] and Parker [28].

3. Results and discussion

3.1. Characterization of samples

Powder XRD patterns of α-$KCoPO_4$ and $RbCoPO_4$, ammonium cobalt and zinc phosphates, and supplementary chemicals ($NH_4H_2PO_4$, CoO, and ZnO) show they are all single phases (see Fig. 1 for XRD patterns of the alkali and ammonium cobalt and zinc phosphate samples). Their calculated lattice parameters (see Table 2) are in agreement with single crystal data or powder data reported elsewhere [1,23]. Since γ-$KCoPO_4$ is an incommensurate phase at room temperature [20], its powder XRD patterns shows some weak peaks that cannot be indexed from the $P2_1/c$ space group. However, the whole XRD pattern of γ-$KCoPO_4$ (Fig. 1A) and its lattice parameters (Table 2) agree well with the powder XRD data reported by Lujan and Schmid [20]. Therefore, this sample is considered to be pure γ-$KCoPO_4$. The description of the structure of γ-$KCoPO_4$ in Lujan and Schmid [20] suggests that this phase has the ABW structure. Consequently, like $NaCoPO_4$ and NH_4MPO_4 (M = Co, Zn) [1,3,4,29], $KCoPO_4$ also exists in ABW (γ-$KCoPO_4$) and HEX (α-$KCoPO_4$) structures. Calculated molar volumes in Table 2 are consistent with the previous reports, that the ABW forms of $KCoPO_4$, NH_4CoPO_4, and NH_4ZnPO_4 are

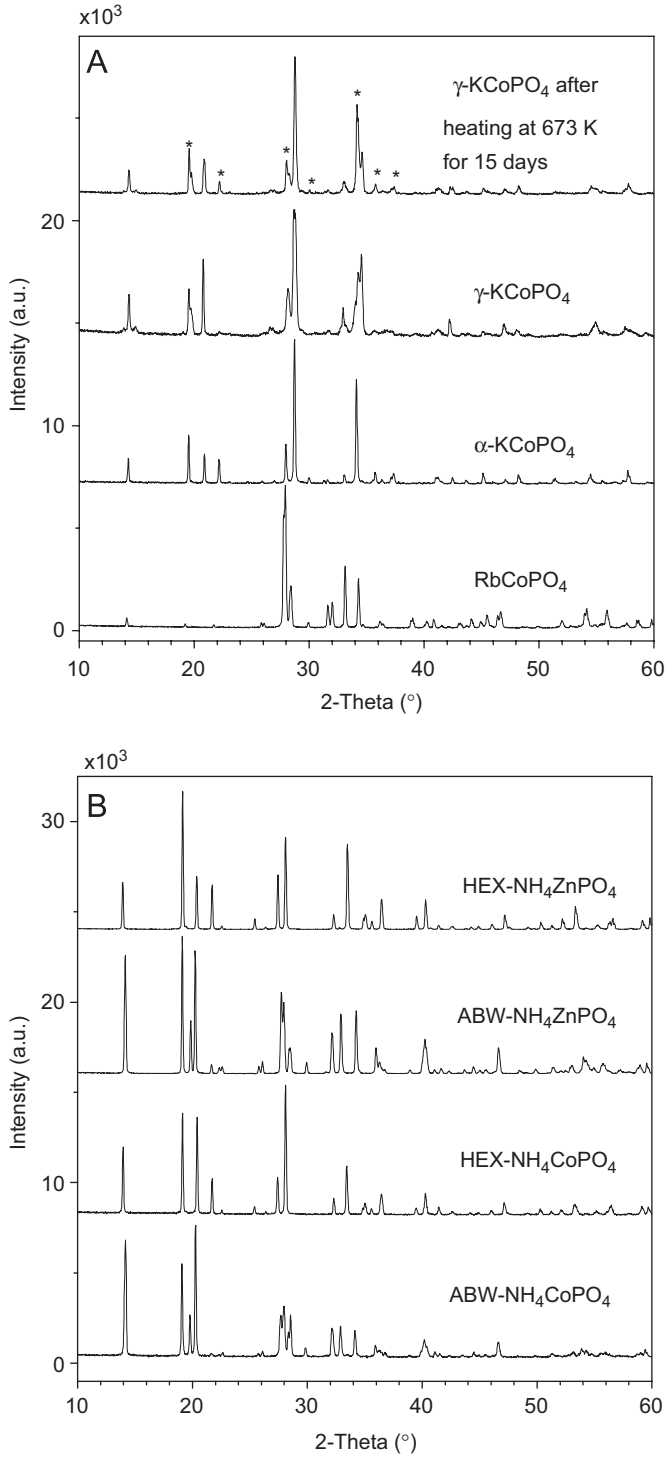

Fig. 1. A/XRD patterns of alkali cobalt phosphate samples. Stars in the pattern of the γ-$KCoPO_4$ sample after heating at 673 K, 15 days indicate the developing peaks belonging to the α-$KCoPO_4$ phase. B/XRD patterns of ammonium cobalt and zinc phosphate samples.

slightly denser than their HEX counterparts [1,3,4,19,20,30].

Microprobe analysis of $KCoPO_4$ and $RbCoPO_4$ reveal their element ratios P/Co/M (M = K, Rb) are close to theoretical: $1/0.99\pm0.02/0.98\pm0.03$ for α-$KCoPO_4$, $1/0.98\pm0.04/1.03\pm0.04$ for γ-$KCoPO_4$, and $1/1.01\pm0.01/1.01\pm0.01$ for $RbCoPO_4$ (uncertainties are standard deviations from at least eight analyzed points). TGA experiments show no weight change within the instrumental error (about $\pm0.1\%$). Chemical compositions of ammonium cobalt and zinc phosphate samples are presented in Table 3. Weight losses from TGA of all samples are consistent with theoretical. The atomic ratios of P/Co or P/Zn for ammonium cobalt and zinc phosphate samples from electron microprobe analysis are close to 1. Therefore, thermodynamic data for all samples are calculated and discussed in terms of their ideal stoichiometries.

3.2. Enthalpies of formation of $KCoPO_4$ and $RbCoPO_4$

All samples dissolved quickly in sodium molybdate melt at 973 K with return to the baseline in about 30 min and gave reproducible values of enthalpies of drop solution (ΔH_{ds}, see Table 4). Enthalpies of drop solution of α-$KCoPO_4$ and γ-$KCoPO_4$ samples in sodium molybdate melt are 149.91 ± 0.67 and 150.93 ± 0.68 kJ mol^{-1}, respectively (averages and two standard deviations of the mean from eight measurements). T-test (a statistics test to determine whether the means of two groups are stastitically different from each other) revealed no significant difference between the two experimental means at 95% confidence level. Consequently, α-$KCoPO_4$ and γ-$KCoPO_4$ are considered to be enthalpically very similar at room temperature and one cannot distinguish which phase is lower in enthalpy. Despite the occurrence of internal domain walls in the ferroelastic γ-$KCoPO_4$ phase, both α-$KCoPO_4$ and γ-$KCoPO_4$ phases are constructed by alternating connections of CoO_4 and PO_4 tetrahedra. Their structures are very similar, the main difference is the orientations of tetrahedra: they are a mixture of up-down (UD) in the sequence UDUDUD and UUUDDD connections in α-$KCoPO_4$, but all UUUDDD in γ-$KCoPO_4$ [1,19,20] (U: up, D: down). The enthalpic similarity of α-$KCoPO_4$ and γ-$KCoPO_4$ reflects the similarity of their structures. Further discussion about thermal behavior of α-$KCoPO_4$ and γ-$KCoPO_4$ is given below.

The thermodynamic cycle A in Table 5 was used to calculate enthalpies of formation from oxides ($\Delta H_{\text{f-ox, 298 K}}$) of $ACoPO_4$ (A = K, Rb). Standard enthalpies of formation ($\Delta H^{o}_{f,298\,K}$, enthalpy of formation from elements) of $ACoPO_4$ were calculated following Eq. (2). All auxiliary values of enthalpies needed for these calculations are in Table 4 (the propagation of errors following Miller and Miller [35] were used to estimate uncertainties for all computed values in this study):

$$\begin{aligned}\Delta H^{o}_{f,298\,K}(ACoPO_4) = {} & \Delta H_{\text{f-ox},298\,K}(ACoPO_4) \\ & + \tfrac{1}{2}\Delta H^{o}_{f,298\,K},(A_2O) \\ & + \Delta H^{o}_{f,298\,K}(CoO) \\ & + \tfrac{1}{2}\Delta H^{o}_{f,298\,K}(P_2O_5). \end{aligned} \quad (2)$$

Table 2
Summary of crystallographic data

Samples	Space group	Lattice parameters				V_m (Å^3)
		a (Å)	b (Å)	c (Å)	β (°)	
α-$KCoPO_4$	$P6_3$	18.2323(3)	18.2323(3)	8.522(6)	90	102.2(1)
γ-$KcoPO_4$	$P2_1/c$	5.232(8)	8.537(7)	10.41(1)	120.57(9)	100.1(2)
$RbCoPO_4$	$P2_1$	8.842(3)	5.412(2)	8.952(3)	90.33(3)	
HEX–NH_4CoPO_4	$P6_3$	10.726(4)	10.726(4)	8.712(3)	90	108.5(1)
ABW–NH_4CoPO_4	$P2_1$	8.781(3)	5.421(2)	8.991(4)	90.32(3)	107.0(1)
HEX–NH_4ZnPO_4	$P6_3$	10.700(9)	10.700(9)	8.714(4)	90	108.0(2)
ABW–NH_4ZnPO_4	$P2_1$	8.790(5)	5.452(4)	8.940(5)	90.35(3)	107.1(1)
CoO	Fm-3m	4.26(1)	4.26(1)	4.26(1)	90	
ZnO	$P6_3mc$	3.24(1)	3.24(1)	5.20(1)	90	
$NH_4H_2PO_4$	I-42d	7.491(3)	7.491(3)	7.538(4)	90	

Numbers in parentheses are estimated standard deviations form JADE refinement [24].
V_m: molar volume of compounds.

Table 3
Atomic ratios from microprobe analysis and weight loss from TGA for NH_4CoPO_4 and NH_4ZnPO_4

Samples	Atomic ratios P/M (M = Co, Zn)	Weight loss (wt%)	
		Experimental	Theoretical
HEX–NH_4CoPO_4	1.00(1)	15.2±0.1	15.14
ABW–NH_4CoPO_4	1.00(1)	15.1±0.1	15.14
HEX–NH_4ZnPO_4	0.98(1)	14.6±0.1	14.63
ABW–NH_4ZnPO_4	1.01(1)	14.6±0.1	14.63

Numbers in parentheses are standard deviations from 8 to 12 analyzed points. Uncertainties of weight loss represent instrumental error.

Table 4
Summary of thermodynamic data used and derived from high-temperature oxide melt calorimetry

Compound	ΔH_{ds} (kJ mol^{-1})	$\Delta H_{f\text{-}ox,\ 298\,K}$ (kJ mol^{-1})	$\Delta H^{o}_{f,298\,K}$ (kJ mol^{-1})
K_2O (cr)	−318.0±3.1 [31]	–	−363.2±2.1 [34]
Rb_2O (cr)	−332.5±9.0 [31]	–	−338.0±8.0 [34]
CoO (cr)	15.35±0.46 [32]	–	−237.9±1.3 [34]
P_2O_5 (cr)	−164.60±0.85 [33]	–	−1504.9±0.5 [34]
α-$KCoPO_4$ (cr)	149.91±0.67	−375.9±1.8	−1547.8±2.5
γ-$KCoPO_4$ (cr)	150.93±0.68	−376.9±1.8	−1548.8±2.5
$RbCoPO_4$ (cr)	148.17±1.42	−381.4±4.8	−1540.7±6.4

ΔH_{ds}, enthalpy of drop solution in sodium molybdate at 973 K (averages from at least seven measurements, uncertainties are two standard deviations of the mean); $\Delta H_{f\text{-}ox,\ 298\,K}$, enthalpy of formation from oxides; and $\Delta H^{o}_{f,298\,K}$, standard enthalpy of formation (enthalpy of formation from elements). Values without cited reference are from this work.

3.3. Thermal behavior and relative stability of $KCoPO_4$ polymorphs

DSC traces for heating α-$KCoPO_4$ and γ-$KCoPO_4$ through $\alpha-\beta$ and $\gamma-\beta$ phase transitions are presented in Fig. 2. Peak temperature of $\alpha-\beta$ and $\gamma-\beta$ phase transitions are 847±1 and 873±1 K, respectively, consistent with those reported elsewhere [19–21]. The cooling traces of α-$KCoPO_4$ and γ-$KCoPO_4$ (see Fig. 2) are similar; both show two exothermic peaks at 825 and 710 K. These exothermic peaks agree well with observation from the optical experiments of Lujan and Schmid [20]. The first exothermic peak (825 K) is associated with the heterogeneity in crystals occurring in the first part of the ferroelastic transformation (starting at 833 K in the optical experiment); the second exothermic peak (710 K) is consistent with the formation of domain walls to finish the ferroelastic phase transition (at 720 K in the optical experiment). XRD of samples after these DSC experiments showed they are γ-$KCoPO_4$ with some additional peaks that could not be identified. Further examination of enthalpies of phase transition on heating and cooling the γ-$KCoPO_4$ sample reveals that the sum of the heat effects on cooling are only 30–60% of that on heating. Thus, the

Table 5
Thermodynamic cycles used for the calculation of enthalpies of formation from oxides

Cycle A: Thermodynamic cycle for the enthalpies of formation from oxides of $ACoPO_4$ (A = K, Rb)	
$ACoPO_4$ (cr, 298 K) → $ACoPO_4$ (sol, 973 K)	$\Delta H_{ds}(ACoPO_4)$
A_2O (cr, 298 K) → A_2O (sol, 973 K)	$\Delta H_{ds}(A_2O)$
CoO (cr, 298 K) → CoO (sol, 973 K)	$\Delta H_{ds}(CoO)$
P_2O_5 (cr, 298 K) → P_2O_5 (sol, 973 K)	$\Delta H_{ds}(P_2O_5)$
1/2 A_2O (cr, 298 K) + CoO (cr, 298 K) + 1/2 P_2O_5 (cr, 298 K) → $ACoPO_4$ (cr, 298 K)	$\Delta H_{f\text{-}ox,\ 298\,K}(ACoPO_4)$
$\Delta H_{f\text{-}ox,\ 298\,K}(ACoPO_4) = 1/2\ \Delta H_{ds}(A_2O) + \Delta H_{ds}(CoO) + 1/2\ \Delta H_{ds}(P_2O_5) - \Delta H_{ds}(ACoPO_4)$	
Cycle B: Thermodynamic cycle for the enthalpies of formation from oxides of NH_4MPO_4 (M = Co, Zn)	
NH_3 (g, 298 K) + 1/2 P_2O_5 (s, 298 K) + 3/2 H_2O (l, 298 K) → $NH_4H_2PO_4$ (s, 298 K)[a]	$\Delta H_{f\text{-}ox,\ 298\,K}(NH_4H_2PO_4)$
$NH_4H_2PO_4$ (s, 298 K) + H^+ (sol, 298 K) → NH_4^+ (sol, 298 K) + H_3PO_4 (sol, 298 K)	$\Delta H_{sln}(NH_4H_2PO_4)$
MO(s, 298 K) + 2 H^+ (sol, 298 K) → M^{2+} (sol, 298 K) + H_2O (sol, 298 K)	$\Delta H_{sln}(MO)$
H_2O (l, 298 K) → H_2O (sol, 298 K)	$\Delta H_{sln}(H_2O)$
NH_4MPO_4 (s, 298 K) + 3 H^+ (sol, 298 K) → NH_4^+ (sol, 298 K) + M^{2+} (sol, 298 K) + H_3PO_4 (sol, 298 K)	$\Delta H_{sln}(NH_4MPO_4)$
NH_3 (g, 298 K) + 1/2 H_2O (l, 298 K) + MO (s, 298 K) + 1/2 P_2O_5 (s, 298 K) → NH_4MPO_4 (s, 298 K)	$\Delta H_{f\text{-}ox,\ 298\,K}(NH_4MPO_4)$
$\Delta H_{f\text{-}ox,\ 298\,K}(NH_4MPO_4) = \Delta H_{f\text{-}ox,\ 298\,K}(NH_4H_2PO_4) + \Delta H_{sln}(NH_4H_2PO_4) + \Delta H_{sln}(MO) - \Delta H_{sln}(NH_4MPO_4) - \Delta H_{sln}(H_2O)$	

[a]Value of enthalpy of formation from ammonia and oxides of $NH_4H_2PO_4$ in Table 6 was calculated following this reaction.

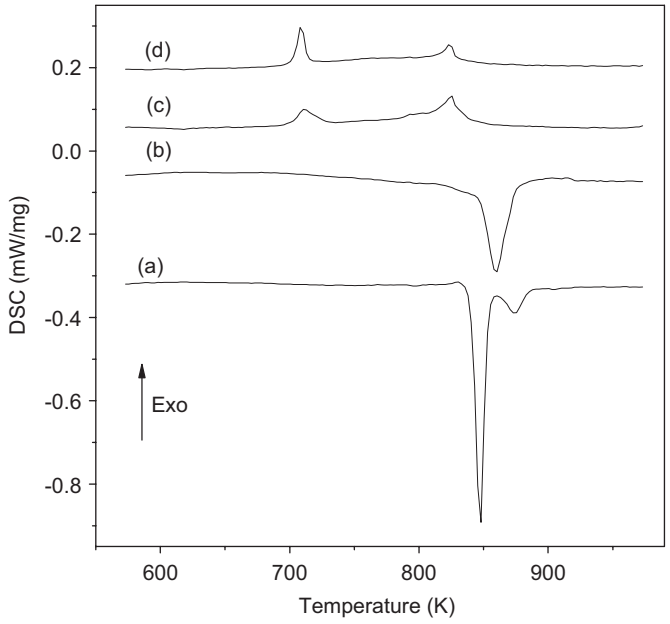

Fig. 2. DSC traces around temperature of ferroelastic phase transition of (a) heating α-$KCoPO_4$, (b) heating γ-$KCoPO_4$, (c) cooling α-$KCoPO_4$, and (d) cooling γ-$KCoPO_4$.

ferroelastic phase transition is sluggish on cooling under the conditions of our DSC experiments.

DSC experiments also help to constrain the relative stability of β-$KCoPO_4$ compared to α-$KCoPO_4$ and γ-$KCoPO_4$. Because of the sluggishness of the phase transitions on cooling, enthalpies of α−β and γ−β phase transitions were derived from heating only. The enthalpy of the α−β $KCoPO_4$ phase transitions is 6.7 ± 0.2 kJ mol^{-1} (average and standard deviation from three measurements) at 850 K. This is similar to the enthalpy of the α−β phase transition of $NaZnPO_4$ [18] (see Table 6). These relatively small enthalpies of transformations reflect the similar geometries of T atoms (T = Co, Zn, P) in the α and β phases of $KCoPO_4$ and $NaZnPO_4$. The endothermic peak associated with the γ−β $KCoPO_4$ phase transition has a shifted baseline before the main peak (see Fig. 2). Consequently, the enthalpy of γ−β $KCoPO_4$ phase transition varies depending on the temperature ranges taken for integrals. It is 6.2 ± 0.6 kJ mol^{-1} for the integral from 713 to 913 K, but 4.7 ± 0.2 kJ mol^{-1} for the integral from 813 to 913 K. Either way, they are relatively large compared with many ferroelastic phase transitions that have ΔH less than 1 kJ mol^{-1} [36–38].

Other experiments were performed by heating α-$KCoPO_4$ and γ-$KCoPO_4$ at 673 K (near the temperature of the ferroelastic phase transition) in a muffle furnace for 15 days. α-$KCoPO_4$ was unchanged after this treatment, but the XRD pattern of γ-$KCoPO_4$ showed the growth of the α-$KCoPO_4$ phase (see Fig. 1A). This suggests α-$KCoPO_4$ is not a metastable phase and it is more stable than γ-$KCoPO_4$ at 673 K. α-$KCoPO_4$ and γ-$KCoPO_4$ are enthalpically essentially the same at room temperature; and entropies of the α, β, and γ phases are not known. The slow transformation at 673 K may suggest that the equilibrium temperature for the γ to α transition may be lower. Further thermodynamic analysis is not possible.

For $KCoPO_4$, the ABW form (γ-$KCoPO_4$) is denser than the HEX form (α-$KCoPO_4$). Thus, the ABW phase could be a high-pressure phase. The ABW phase transforms to the HEX phase at 673 K at atmosphere pressure. Thus, the less dense HEX phase appears to be a high-temperature phase, implying a positive dP/dT for any possible ABW–HEX transition. The existence of β-$KCoPO_4$ at higher temperature further complicates possible phase relations.

3.4. Enthalpies of solution of NH_4CoPO_4 and NH_4ZnPO_4 in 5.0 M HCl and relative stability of their HEX and ABW structures

All ammonium cobalt and zinc phosphate samples and supplementary chemicals ($NH_4H_2PO_4$, CoO, and ZnO)

Table 6
Summary of the thermodynamic of phase transitions of cobalt and zinc phosphate frameworks

Compounds	Transition	T (K)	ΔH (kJ mol^{-1})	ΔS (J K^{-1} mol^{-1})
$NaCoPO_4$ [16]	$\alpha \leftrightarrow \beta$[a]	1006	17.6 ± 1.3[f]	17.5 ± 1.3
$NaCoPO_4$ [16]	red $\rightarrow \alpha$[b]	827	-17.4 ± 6.9[f]	
$KCoPO_4$	$\alpha \rightarrow \beta$[c]	847	6.7 ± 0.2[g]	7.9 ± 0.2[h]
$KCoPO_4$	$\gamma \rightarrow \beta$[c]	813–913[e]	4.7 ± 0.2[g]	5.5 ± 0.2[h]
		713–913[e]	6.2 ± 0.2[g]	7.3 ± 0.2[h]
$KCoPO_4$	$\gamma \rightarrow \alpha$[c]	Partially transformed at 673	~ 0[f]	
NH_4CoPO_4	HEX $\rightarrow$ ABW[c,d]	–	2.9 ± 0.5[f]	
$NaZnPO_4$ [18]	$\alpha \leftrightarrow \beta$[a]	1160	6.8 ± 0.1[g]	5.9 ± 0.1
NH_4ZnPO_4	HEX $\rightarrow$ ABW[c,d]	–	3.0 ± 0.1[f]	

Data without cited references are from this work.
[a]Reversible transition.
[b]Irreversible transition.
[c]Not clear whether reversible or irreversible.
[d]No phase transition observed on DSC.
[e]Enthalpies of the $\gamma-\beta$ $KCoPO_4$ transformation depend on temperature range chosen for DSC baseline.
[f]Values derived from enthalpies of drop solution (in high temperature oxides melt calorimetry) or solution (in acid solution calorimetry).
[g]Values derived from DSC experiments.
[h]Reversible transition assumed for entropy calculations.

Table 7
Summary of thermodynamic data used and derived from acid solution calorimetry

Compound	ΔH_{sln} (kJ mol^{-1})	$\Delta H_{f\text{-}ox,\ 298\,K}$ (kJ mol^{-1})	$\Delta H^{\circ}_{f,298\,K}$ (kJ mol^{-1})
ZnO (cr)	-71.90 ± 0.11	–	-350.5 ± 0.3 [34]
CoO (cr)	-105.82 ± 0.36	–	-237.9 ± 1.3 [34]
H_2O (l)	-0.5[a]	–	-285.83 ± 0.04 [34]
NH_3 (g)	–	–	-45.9 ± 0.4 [34]
P_2O_5 (s)	–	–	-1054.9 ± 0.5 [34]
$NH_4H_2PO_4$ (cr)	25.26 ± 0.19	-218.0 ± 1.0[b]	-1445.07 ± 0.8 [39]
HEX–NH_4CoPO_4 (cr)	-52.70 ± 0.24	-245.3 ± 1.0	-1424.5 ± 1.7
ABW–NH_4CoPO_4 (cr)	-55.59 ± 0.39	-242.5 ± 1.1	-1421.6 ± 1.8
HEX–NH_4ZnPO_4 (cr)	-10.79 ± 0.06	-253.3 ± 1.0	-1545.1 ± 1.1
ABW–NH_4ZnPO_4 (cr)	-13.75 ± 0.08	-250.4 ± 1.0	-1542.1 ± 1.1

ΔH_{sln}, enthalpy of solution in 5 M HCl solution at 298 K (uncertainties of those experimental enthalpies are two standard deviations of the mean); $\Delta H^{\circ}_{f,298\,K}$, standard enthalpy of formation (enthalpy of formation from elements); $\Delta H_{f\text{-}ox,\ 298\,K}$, enthalpy of formation from oxides and NH_3. Numbers without cited references are from this work.
[a]Enthalpy of solution of water ($\Delta H_{sln}(H_2O)$, enthalpy of dilution), expressed by the reaction: H_2O (l, 298 K) $\rightarrow$ H_2O (sol, 298 K), is varied on concentration and composition of solutions. Value in this paper refers to the enthalpy of a limited dilution of a 5 M HCl solution associated with our experimental conditions. Data for this calculation were taken from Parker [28], small uncertainty was neglected for convenience.
[b]This value refers to the enthalpy of reaction (*) in Table 5.

dissolved well in 5 M HCl with a return to baseline in 60–70 min and provided reproducible enthalpies of solution (ΔH_{sln}, see Table 7). Relative stability of HEX and ABW structures of ammonium cobalt and zinc phosphates at 298 K ($\Delta H_{HEX-ABW,\ 298\,K}$) were derived following Eq. (3) and appropriate values of enthalpies of solution in Table 7:

$$\Delta H_{HEX-ABW,298\,K} = \Delta H_{sln}(ABW) - \Delta H_{sln}(HEX). \quad (3)$$

At room temperature, the HEX phases are 2.9 ± 0.5 and 3.0 ± 0.1 kJ mol^{-1} more stable than the ABW phases for NH_4CoPO_4 and NH_4ZnPO_4, respectively. These enthalpy differences are similar and relatively small. Both compounds with the ABW structure are slightly denser but higher in enthalpy than the HEX ones. This behavior may be related to the relatively small size of NH_4^+ ions in the eight ring channels of the ABW frameworks, leading to the distortion of NH_4^+ ions and looser hydrogen bonds between NH_4^+ ions and the frameworks, as discussed elsewhere [1,3]. Since the enthalpically less stable form (ABW) is the denser form, this implies that, if both ABW and HEX forms have any equilibrium stability field, the ABW form would be stable at high temperature and high pressure, and the dP/dT for the HEX $\rightarrow$ ABW transition would be negative. $KCoPO_4$ also exists as HEX (α-$KCoPO_4$) and ABW (γ-$KCoPO_4$) polymorphs, but they do not appear to follow the same P–T behavior (see above) as ammonium cobalt and zinc phosphate. The reason for the different slopes (and therefore enthalpies) for the potassium and ammonium compounds is not known. One

can speculate that hydrogen bonding in the ammonium compounds may play a role.

3.5. Enthalpies of formation of NH_4CoPO_4 and NH_4ZnPO_4

Enthalpies of formation from ammonia and oxides of NH_4MPO_4 (M = Co, Zn) are represented by reaction (4). This is a useful formulation to discuss acid–base interactions in these materials. For convenience, we simply call these quantities enthalpies of formation from oxides ($\Delta H_{\text{f-ox, 298 K}}$):

$$NH_3(g, 298\,K) + \tfrac{1}{2}H_2O(l, 298\,K) + MO(cr, 298\,K) + \tfrac{1}{2}P_2O_5(cr, 298\,K) \rightarrow NH_4MPO_4(cr, 298\,K) \quad \Delta H_{\text{f-ox,298 K}}(NH_4MPO_4). \tag{4}$$

Thermodynamic cycle B in Table 5 and auxiliary values of enthalpies in Table 7 were applied for the calculation of enthalpies of formation from oxides of NH_4MPO_4. These, and standard enthalpies of formation ($\Delta H^{\circ}_{\text{f,298 K}}$, enthalpy of formation from elements) of NH_4MPO_4, calculated following Eq. (5), are shown in Table 7:

$$\Delta H^{\circ}_{\text{f,298 K}}(NH_4MPO_4) = \Delta H_{\text{f-ox,298 K}}(NH_4MPO_4) + \Delta H^{\circ}_{\text{f,298 K}}(NH_3) + \tfrac{1}{2}\Delta H^{\circ}_{\text{f,298 K}}(H_2O) + \tfrac{1}{2}\Delta H^{\circ}_{\text{f,298 K}}(P_2O_5)\Delta H^{\circ}_{\text{f,298 K}}(MO). \tag{5}$$

3.6. Relationships among enthalpies of formation from oxides, acid–base interactions, and structures of cobalt and zinc phosphates compared with aluminosilicates

In a previous paper [16], we highlighted that, comparing $NaCoPO_4$ and $NaAlSiO_4$ with related structures, acid–base interactions in $NaCoPO_4$ are much stronger than in $NaAlSiO_4$ since the acidity difference between CoO and P_2O_5 is bigger than that between Al_2O_3 and SiO_2. Here, enthalpies of formation from oxides of ACoPO$_4$ and AAlSiO$_4$ (A = Na, K, Rb, all with similar frameworks) are plotted against the acidities of alkaline oxides (Smith's scale [40]) in Fig. 3. The graph exhibits not only analogous trends in enthalpies of formation from oxides for aluminosilicates and cobalt phosphates but also good correlations between enthalpy of formation from oxides and acidity of alkali oxides ($R^2 = 0.99$ for both lines). The stronger the basicity (weaker acidity) of the alkali oxide, the more exothermic is the enthalpy of formation from oxides, reflecting the stronger acid–base interactions. The graph also shows the less exothermic enthalpies of formation from oxides of aluminosilicates compared to cobalt phosphates, confirming our previous reasoning that acid–base interactions in aluminosilicates are significantly weaker than those in cobalt phosphates. It is clear that there is a strong relationship between enthalpy of formation from oxides and acid–base interaction in alkali cobalt phosphates and alkali aluminosilicates.

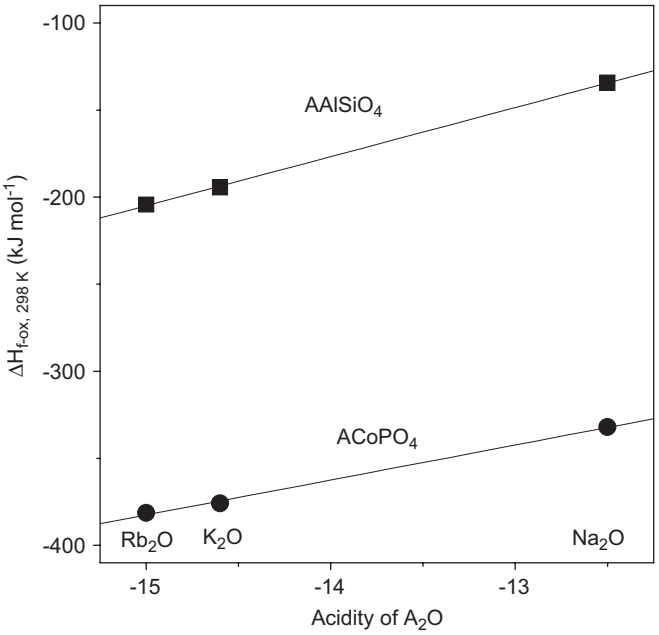

Fig. 3. Enthalpies of formation from oxides ($\Delta H_{\text{f-ox, 298 K}}$) of alkali cobalt phosphates (ACoPO$_4$) and alkali aluminosilicates (AAlSiO$_4$) as functions of the acidity of alkali oxides (alkali A = Na, K, and Rb; Co, P, Al, and Si are all in tetrahedral coordination). Uncertainties of enthalpies are approximately the same as the sizes of the symbols in the graph. Acidity of Na_2O, K_2O, and Rb_2O are −12.0, −14.6, and −15.0, respectively [40]. Enthalpies of formation from oxides of $KCoPO_4$ and $RbCoPO_4$ are in Table 4, those of β-$NaCoPO_4$, $NaAlSiO_4$ nepheline, and $KAlSiO_4$ kalsilite are -332.1 ± 2.5 kJ mol^{-1} [16], -134.4 ± 4.0 kJ mol^{-1} [15], and -194.6 ± 3.5 kJ mol^{-1} [15], respectively. Enthalpy of formation from oxides of $RbAlSiO_4$ is extrapolated to be -204.3 ± 5 kJ mol^{-1}, data for this estimation are taken from Navrotsky and Tian [15].

The relationship between acid–base interaction and enthalpy of formation from oxides of alkali cobalt phosphates can be extended to ammonium cobalt phosphates. Eqs. (6) and (7) represent the formations of alkali cobalt phosphates (ACoPO$_4$) and ammonium cobalt phosphates:

$$\tfrac{1}{2}A_2O(cr, 298\,K) + CoO(cr, 298\,K) + \tfrac{1}{2}P_2O_5(cr, 298\,K) \rightarrow ACoPO_4(cr, 298\,K), \tag{6}$$

$$NH_3(g, 298\,K) + \tfrac{1}{2}H_2O(l, 298\,K) + CoO(cr, 298\,K) + \tfrac{1}{2}P_2O_5(cr, 298\,K) \rightarrow NH_4CoPO_4(cr, 298\,K). \tag{7}$$

Alkali oxide (A_2O) in the formation of alkali cobalt phosphate is replaced by ammonia and water for the formation of ammonium cobalt phosphate (see Eqs. (6) and (7)). Both ammonia and water are weaker bases than alkali oxides (Na_2O, K_2O, and Rb_2O). Thus, acid–base interactions in ammonium cobalt phosphates are weaker than those in alkali cobalt phosphates and enthalpies of formation from oxides of ammonium cobalt compared are less exothermic than those of alkali cobalt phosphates (see values in Table 6 and footnotes of Fig. 3). Fig. 4A

demonstrates the extrapolation of the linear relationship in Fig. 3 to ammonium cobalt phosphates. Acidity of a hypothetical "ammonium oxide" ($(NH_4)_2O$) can then be estimated to be about −6.7 in this extrapolation. This value is less negative than the acidity of alkali oxides, even Li_2O (−9.2, in Smith's scale [40]), and is reasonable for the acidity of a weak base.

The relationship between acid and base interactions and enthalpy of formation from oxides of compounds is strengthened when comparing the thermodynamic data of cobalt and zinc phosphates. The difference of enthalpies of formation from oxides of NH_4CoPO_4 and NH_4ZnPO_4 are small, about 8 kJ mol^{-1} (see Table 6). This similarity reflects similar acid–base interactions in cobalt and zinc phosphate compounds and agrees with the similar acidity of CoO and ZnO (−3.8 and −3.2, respectively, in Smith's scale [40] that ranges from −15.2 for Cs_2O, the strongest base, to 11.5 for Cl_2O_7, the strongest acid). This is also consistent with our findings in a previous study [18], that acidity of CoO and ZnO are similar, and β-$NaCoPO_4$ and α-$NaZnPO_4$ (both having Co and Zn in tetrahedral coordination) have similar enthalpies of formation from oxides. Thermodynamic data of those zinc phosphates are plotted as open circles in Fig. 4A to display the similar enthalpies of cobalt and zinc phosphate frameworks.

It is interesting to emphasize that plotting enthalpy of formation from oxides of alkali cobalt phosphates against the ionic potential of alkali ions (Z/r: charge divided by ionic radius) also gives a similar linear relationship as those with the acidity of alkali oxides (Fig. 4B). However, ionic potential of NH_4^+ is similar to that of K^+, while the enthalpies of formation of ammonium cobalt phosphates are much less exothermic than those of $KCoPO_4$. Thus, the ammonium compounds do not follow the same trend as the alkali ones. Enthalpy of formation from oxides of $ACoPO_4$ ($A = NH_4$, Na, K, and Rb) correlates better with acid–base interaction (if creatable value of acidity is chosen for "$(NH_4)_2O$", see above) rather than with ionic potential of A^+ ions.

Since the enthalpy differences among various polymorphs of aluminosilicates, cobalt phosphates, and zinc phosphates are often less than 10 kJ mol^{-1} [11–15, this work], it is clear that acid–base interactions dominate the enthalpy of formation of these compounds, while their structures play a smaller role. The extensive polymorphism seen in cobalt phosphates, zinc phosphate, and aluminosilicates is allowed by small energy differences among polymorphs.

Lithium oxide is a stronger base than ammonia and water (or "$(NH_4)_2O$"); therefore it is reasonable to expect that acid–base interactions in $LiCoPO_4$ are intermediate between those in NH_4CoPO_4 and $NaCoPO_4$. However, $LiCoPO_4$ does not possess any structures related to the HEX or ABW frameworks seen in NH_4CoPO_4 or $NaCoPO_4$. It is known only in the olivine structure in which cobalt is in octahedral environment [42]. For the small Li^+ ion, an open framework structure with Li^+ in large cavities is apparently not stable, and a more denser structure with both Li^+ and Co^{2+} in octahedral coordination is adopted. Furthermore, ionic radii of Co^{2+} and Zn^{2+} are similar, acidity of CoO and ZnO are similar, but $LiZnPO_4$ is known in various structures and none of them

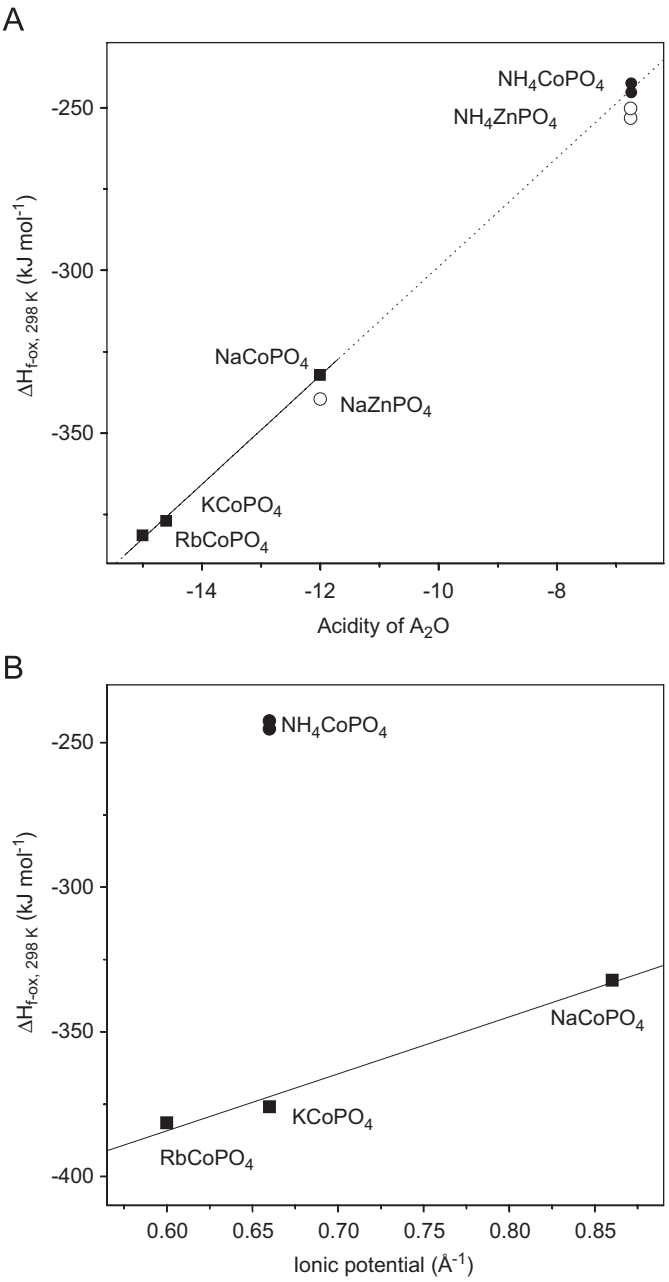

Fig. 4. (A) Extrapolation of the linear relationship between the enthalpy of formation from oxides of alkali cobalt phosphates and the acidity of alkali oxides in Fig. 3 to ammonium cobalt phosphates (showed by dotted line) displays weaker acid–base interaction in ammonium cobalt phosphates than in alkali cobalt phosphates. Thermodynamic data for zinc phosphate frameworks (open circles) are analogous to those of cobalt phosphate frameworks. Enthalpies of formation from oxides of α-$NaZnPO_4$ is -339.6 ± 2.6 kJ mol^{-1} [18]. (B) Enthalpies of formation from oxides of alkali cobalt phosphates exhibit a linear relationship with ionic potential of alkali ions, but NH_4CoPO_4 does not follow that trend. Data for the calculation of ionic potential (Z/r) were taken from Jenkins and Thakur (cited in [41]) and Shannon (cited in [41]).

is similar to $LiCoPO_4$. All the known frameworks of $LiZnPO_4$ are constructed from ZnO_4 and PO_4 tetrahedra [43–45]. The δ_1 form of $LiZnPO_4$ possesses a cristobalite like structure, which is related to the HEX structure of NH_4ZnPO_4 [44]. These differences emphasize that, although acid–base chemistry may dominate the magnitude of the enthalpy of formation, other factors, such as ionic radius and electron configuration of the transition metal, help determine the actual structures formed.

4. Conclusion

α-$KCoPO_4$ and γ-$KCoPO_4$ are enthalpically equivalent at room temperature. At 673 K, γ-$KCoPO_4$ transforms slowly to α-$KCoPO_4$. The high-temperature phase β-$KCoPO_4$ is 5–7 kJ mol^{-1} less enthalpically stable than γ-$KCoPO_4$ and α-$KCoPO_4$ at 850 K. HEX phases of NH_4MPO_4 ($M = Co$, Zn) are 3 kJ mol^{-1} more enthalpically stable than ABW phases. There is a strong correlation between enthalpy of formation from oxides and acid–base interaction in cobalt phosphate, zinc phosphate, and aluminosilicate frameworks, but other factors may determine the actual structures formed.

Acknowledgments

This work was supported by the National Science Foundation under Grant DMR 06-01892. We thank Sarah Roeske and Sean Mulcahy for microprobe analysis and John Neil and Lan Wang for providing the CoO sample.

References

[1] P. Feng, X. Bu, S.H. Tolbert, G.D. Stucky, J. Am. Chem. Soc. 119 (1997) 2497–2504.
[2] H.Y. Ng, W.T.A. Harrison, Microporous Mesoporous Mater. 23 (1998) 197–202.
[3] X. Bu, P. Feng, T.E. Gier, G.D. Stucky, Zeolites 19 (1997) 200–208.
[4] W.T.A. Harrison, A.N. Sobolev, M.L.F. Phillip, Acta Crystallogr. C 57 (2001) 508–509.
[5] J. Chen, R.H. Jones, S. Natarajan, M.B. Hursthouse, J.M. Thomas, Angew. Chem. Int. Ed. Engl. 33 (1994) 639–640.
[6] H.-M. Yuan, J.-S. Chen, G.-S. Zhu, J.-Y. Li, J.-H. Yu, G.-D. Yang, R.-R. Xu, Inorg. Chem. 39 (2000) 1476–1479.
[7] W.T.A. Harrison, Acta Crystallogr. E 57 (2001) m248–m250.
[8] F.O.M. Gaslain, A.M. Chippindale, C. R. Chimie 8 (2005) 521–529.
[9] S. Neeraj, S. Natarajan, J. Phys. Chem. Solids 62 (2001) 1499–1505.
[10] S. Natarajan, S. Neeraj, A. Choudhury, C.N.R. Rao, Inorg. Chem. 39 (2000) 1426–1433.
[11] P.M. Piccione, C. Laberty, S. Yang, M.G. Camblor, A. Navrotsky, M.E. Davis, J. Phys. Chem. B 104 (2000) 10001–10011.
[12] P.M. Piccione, B.F. Woodfield, J. Boerio-Goates, A. Navrotsky, M.E. Davis, J. Phys. Chem. B 105 (2001) 6025–6030.
[13] P.M. Piccione, S. Yang, A. Navrotsky, M.E. Davis, J. Phys. Chem. B 106 (2002) 3629–3638.
[14] J. Boerio-Goates, R. Stevens, B.K. Hom, B.F. Woodfield, P.M. Piccione, M.E. Davis, A. Navrotsky, J. Chem. Thermodyn. 34 (2002) 205–227.
[15] A. Navrotsky, Z.-R. Tian, Chemistry (Weinheim an der Bergstrasse, Germany). 7 (2001) 769–774.
[16] S.-N. Le, H.W. Eng, A. Navrotsky, J. Solid State Chem. 179 (2006) 3731–3738.
[17] ⟨http://www.iza-structure.org/databases/⟩.
[18] S.-N. Le, A. Navrotsky, Energetics of phosphate frameworks containing zinc and cobalt: $NaZnPO_4$, $NaH(ZnPO_4)_2$, $NaZnPO_4 \cdot H_2O$, $NaZnPO_4 \cdot 4/3H_2O$, and $NaCo_xZn_{1-x}PO_4 \cdot 4/3H_2O$, J. Solid State Chem. (Article in press, accepted manuscript.).
[19] M. Lujan, F. Kubel, H. Schmid, Z. Naturforsch. B: Chem. Sci. 49 (1994) 1256–1262.
[20] M. Lujan, H. Schmid, Ferroelectrics 175 (1996) 41–50.
[21] G. Engel, Neues Jahbr. Min. Abh. 127 (1976) 197–211.
[22] L. Wang, A. Navrotsky, R. Stevens, B.F. Woodfield, J. Boerio-Goates, J. Chem. Thermod. 35 (7) (2003) 1151–1159.
[23] Inorganic Crystal Structure Database, National Institute of Standards and Technology, version 1.3.3, 2004.
[24] MDI Materials Database, JADE 6.
[25] A. Navrotsky, in: C.M. Gramaccioli (Ed.), Energy Modelling in Minerals, University Textbook, Eotvos University Press, Budapest, 2002, p. 5.
[26] A. Navrotsky, Phys. Chem. Miner. 24 (1997) 222.
[27] National Bureau of Standards Certificate—Standard Reference Material 1655.
[28] V.B. Parker, Thermal Properties of Uni-univalent Electrolytes, National Bureau of Standards (US), No. 2, 1965, p. 58.
[29] A.M. Chippindale, A.R. Cowley, J. Chen, Q. Gao, R. Xu, Acta Crystallogr. C 55 (1999) 845–847.
[30] M.T. Averbuch-Pouchot, A. Durif, Mater. Res. Bull. 3 (1968) 719–722.
[31] S.V. Ushakov, A. Navrotsky, J.M. Farmer, L.A. Boatner, J. Mater. Res. 19 (2004) 2165–2175.
[32] M. Wang, A. Navrotsky, Solid State Ionics 166 (2004) 167–173.
[33] S.V. Ushakov, K.B. Helean, A. Navrotsky, L.A. Boatner, J. Mater. Res. 16 (2001) 2623–2633.
[34] R.A. Robie, B.S. Hemingway, Thermodynamic Properties of Minerals and Related Substances at 298.15 K and 1 bar (105 P) Pressure and at High Temperatures; Geological Survey Bulletin No. 2134, US Government Printing Office, Washington, DC, 1995.
[35] J.N. Miller, J.C. Miller, Statistics and Chemometrics for Analytical Chemistry, fourth ed, Prentice-Hall, New York, 2000.
[36] F.J. Romero, M.C. Gallardo, J. Jimenez, J.D. Cerro, Thermochim. Acta 372 (2001) 25–31.
[37] C.W.A. Paschoal, A.P. Ayala, I. Guedes, R.L. Moreira, J.-Y. Gesland, Solid State Commun. 129 (2004) 539–543.
[38] S. Haussuehl, Acta Crystallogr. A 34 (1978) 965–968.
[39] D.D. Wagman, W.H. Evans, V.B. Parker, R.H. Schumm, I. Halow, S.M. Bailey, K.L. Churney, R.L. Nuttall, The NBS Tables of Chemical Thermodynamic Properties—Selected Values for Inorganic and C_1 and C_2 Organic Substances in SI Units, American Chemical Society, Washington, DC, 1982.
[40] D.W. Smith, J. Chem. Educ. 64 (1987) 480–481.
[41] J.E. Huheey, E.A. Keiter, R.L. Keiter, Inorganic Chemistry—Principles of Structure and Reactivity, 4th ed, Harper Collins College Publishers, New York, 1993.
[42] P. Deniard, A.M. Dulac, X. Rocquefelte, V. Grigorova, O. Lebacq, A. Pasturel, S. Jobic, J. Phys. Chem. Solids 65 (2004) 229–233.
[43] L. Elammari, B. Elouadi, Acta Crystallogr. Cryst. Struct. Commun. C 45 (1989) 1864–1867.
[44] T.R. Jensen, P. Norby, P.C. Stein, A.M.T. Bell, J. Solid State Chem. 117 (1995) 39–47.
[45] X. Bu, T.E. Gier, G.D. Stucky, Acta Crystallogr. Cryst. Struct. Commun. C 52 (1996) 1601–1603.